

The C-V investigation of light-related properties of porous silicon/crystalline silicon structure

E. Pinèk, M. Jergel, J. Bartoš

Institute of Physics of the Slovak Academy of Sciences, Dúbravská cesta 9, 842 28 Bratislava, Slovakia

C. Falcony

Physics Department, CINVESTAV del I.P.N., Apdo. Postal 14-740, 07000, México D.F., México

M. Kuèera

Institute of Electrical Engineering of the Slovak Academy of Sciences, Dúbravská cesta 9, 842 39 Bratislava, Slovakia

This paper presents a study of porous silicon layer of $\approx 1 \mu\text{m}$ thickness, formed electrolytically in crystalline p-Si, by X-ray diffraction at grazing incidence, photoluminescence (PL) at 6 K and room temperature, C-V measurements, and charge version of deep level transient spectroscopy (DLTS). The C-V measurements performed at LN_2 and room temperatures showed that the electrical properties of the structure are extraordinary sensitive to light illumination and air humidity. Namely, a large hysteresis of the C-V curves is completely lost on the light illumination. The sensitivity of the DLTS signal to light illumination and the temporal stability of the PL spectra at room temperature are illustrated, too. Common features with the optical properties of the amorphous Si:H/crystalline Si structure (Staebler-Wronski effect) are discussed.

1. Introduction

There is still a lack of basic knowledge regarding the interplay between the structure and composition of porous silicon and its optical activity. There are several factors hampering such a study like heterogeneity of the layers, increased chemical reactivity at room temperature in the air, characteristic sizes of the optically active structures, penetration depths of probing light rays (usually, the layers are thicker than the region from which the response is recorded) etc. We refer to an exhaustive review paper by Cullis et al.¹ and Ph.D. thesis by Anderson² presenting the application of porous silicon samples as a humidity sensor based on the effect of the water vapour condensation in the silicon pores.

Parameters such as Fermi level, flat-band voltage, surface potential, deep level hole traps and acceptor density will be presented. These were calculated from the C-V measurements performed on metal/porous silicon/crystalline silicon structures with different vacuum and temporal histories and processed by light exposure.

2. Experimental details

The porous silicon (PS) layers were prepared by anodic etching using an electrolyte containing 40% solution of HF and ethanol (1:3). The constant current density mode (below 5 mAcm^{-2}) was used in the electrochemical etching procedure leading to the formation of $\sim 1 \mu\text{m}$ thick porous layer. The etched crystalline silicon was (100) oriented p-type wafer with the acceptor concentration of the $\sim 10^{16} \text{ cm}^{-3}$ order. Ohmic metal

contacts (either Al or Au) were formed on both the top and bottom parts of the PS/c-Si structure. The X-ray diffraction at grazing incidence (XRDGI) was measured on a Siemens D 5000 diffractometer equipped with a special grazing incidence attachment using CuK_α radiation. The LiF monochromator was placed in the secondary beam. The grazing angle α was set between 0.5° and 3° . The XRDGI patterns of PS samples contain both 111 and 311 reflections at lower grazing angles coming from the outermost layer region (Fig.1 and Fig.2). The sharpness of the 111 reflection at $\alpha=0.5^\circ$ indicates^{1,3} that PS layer consists of nanocrystals of the size of 60 nm as calculated from the Scherrer equation. The 111 reflection is absent in the diffraction pattern at $\alpha=1.5^\circ$. The silicon crystal lying below the PS layer is characterized by 311 reflection which is the most intense at the grazing angle $\alpha=2.5^\circ$.

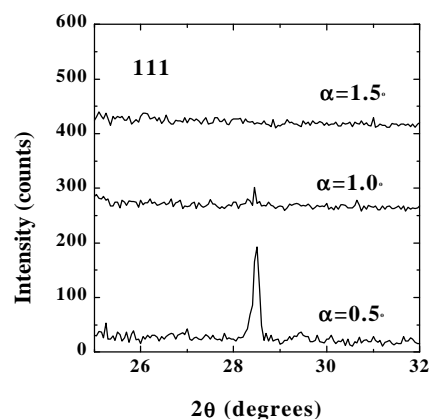


Fig. 1. XRDGI patterns of typical 111 reflection (see Ref. 1) coming from the uppermost part of the PS layer. The angles of incidence are indicated at the curves.

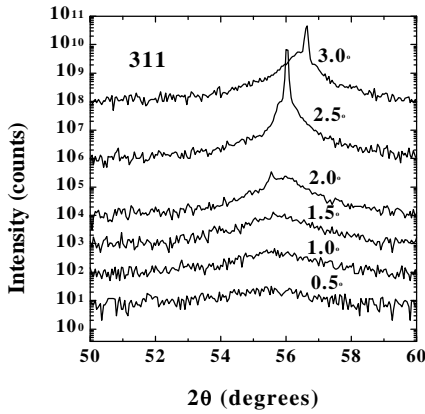


Fig. 2. Evolution of the XRDGI patterns of an unexpected maximum (see Ref. 3) corresponding to 311 reflection. The angles of incidence are indicated at the curves.

The photoluminescence (PL) measurements were done at both 6 K and 300 K using an Ar laser irradiating at 488 nm and a standard lock-in technique with Ga and/or Si photovoltaic detectors. The luminescence spectrum measured at 6 K contains only one IR band at ~1.1 eV. The low-porosity layers have this type of luminescence response¹. An intense illumination of hydrogen containing materials affects also the structure of defects and therefore the PL spectrum can be modified in time. The room temperature PL measurements are illustrated in Fig.3 where the temporal stability of the spectra recorded is presented.

Improved feedback charge measurements in time domain were used for the capacitance measurements of the MIS diodes as a function of gate bias U_g . The capacity of the structure is given by the relation $C=C_F(Du/Du_0)$ where $C_F=330$ pF and $Du_0=20$ mV. The sampling time was set to 200 μ s. The Q-DLTS spectra were recorded in the C_0 mode with the samples positioned at $t_1=0.5$ ms and $t_2=1$ ms with respect to the leading edge of the square wave of the amplitude $DU=50$ mV.

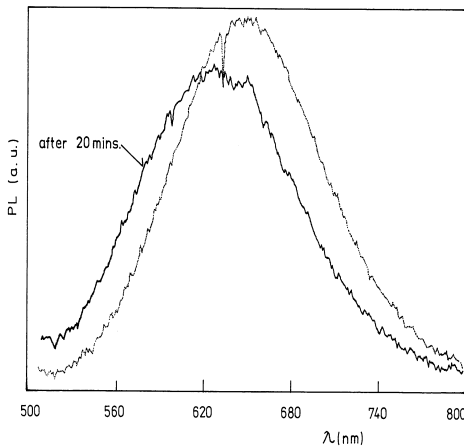


Fig. 3. PL spectra measured at room temperature. They illustrate non-reversible change after 20 minute irradiation of the sample with focused $1Wcm^{-2}$ laser beam.

3. Results and discussion

The dominant set of C-V dependences is shown in Fig.4. The curves are marked by the numbers which correspond to the following conditions of measurements :
 1 - the sample was kept at the temperature of 300 K, under the vacuum of 5 Pa, in dark;
 2 - at 300 K, air conditions, in dark;
 3 - at 300 K, air conditions, in the visible light;
 4 - at 100 K, under the vacuum, in dark.

The basic electronic parameters of the structure investigated were determined from the curves no. 1-4. The acceptor density N_a and flat band voltage U_{FB} in the depletion approximation are given as

$$N_a = \frac{2}{q e_s} \left(\frac{dC^{-2}}{dU_g} \right)^{-1} \tag{1}$$

where q , e_s and U_g are elementary charge, semiconductor permittivity and gate voltage, respectively, and

$$U_{FB} = U_0 + j_0 \tag{2}$$

where

$$j_0 = \frac{q N_a e_s}{2 C_d^2}, \tag{3}$$

C_d being the accumulation capacity and U_0 being determined by the interception of the dC^{-2}/dU_g dependence with U_g axis.

The thermal activation energy E_t for the deep level trap with respect to the top of the semiconductor valence band is determined as

$$E_t = E_F + j_s \tag{4}$$

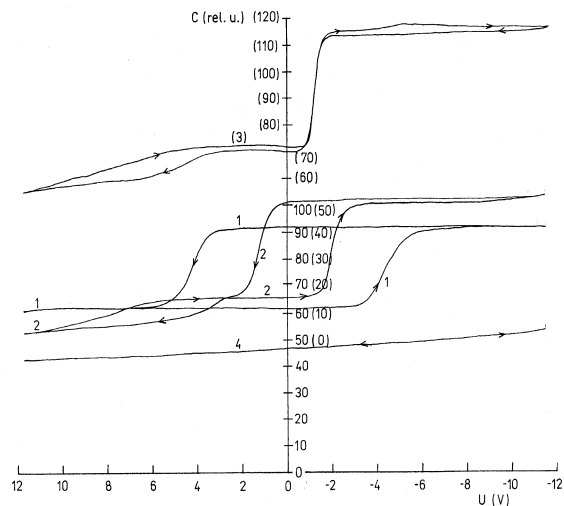


Fig. 4. Set of C-V curves measured under different light and vacuum conditions as described in the text.

where j_s is the surface potential and E_F is the semiconductor Fermi level given as

$$E_F = kT \ln \left(\frac{N_v}{N_a} \right) \quad (5)$$

From a careful inspection of Fig.4 it can generally be stated that the clock-wise C-V hysteresis increases and the slope of the C-V curves decreases when the light is switched off (i.e. when the samples are not illuminated). The air pressure in the cryostat used is lowered and the sample is cooled. Higher density of the interface states generated leads to smoother C-V curves as well as to a larger hysteresis. Simultaneously with the continuous spectrum of the interface states sensitive to the sample exposure during the C-V measurements, the signal from a discrete deep level is observed on the C-V curve (see the step on the curve no.4 in Fig.4).

The C-V hysteresis depends also on the non-equilibrium conditions. The non-equilibrium in voltage sweep increases as the temperature is lowered, light is switched off, and charged gas atoms (ions) escape. These parameters are responsible for the hysteresis observed. However, the slope of C-V curve is determined also by two further parameters at least, namely by the density of the acceptors in the semiconductor crystal part at the interface with the modified layer and by the density of interface states. Moreover, the thickness of the porous layer calculated from the accumulation capacity increases as the gas pressure in cryostat is lowered, light is switched off and the sample is cooled down. The permittivity of the porous layer alters, too, because of the change in the air humidity². We suppose that this effect can be explained more precisely as the consequence of the free charge concentration reduction in the layer with the same result, namely the thickening of the PS layer and decrease of the PS permittivity value.

The gate voltage U_g in p-type MIS structure with homogeneous density of acceptors N_a [cm^{-3}] and homogeneous density of interface states N_{ss} [$\text{cm}^{-2}\text{eV}^{-1}$] throughout the gap is given as

$$U_g - U_{FB} = \frac{qN_a W + C_{ss} j_s}{C_d} + j_s \quad (6)$$

where $q=1.602 \times 10^{-19}$ C, W is the space charge region width in the semiconductor, $C_{ss}=q^2 N_{ss}$, $C_d=\epsilon_d/d$, ϵ_d is insulator permittivity, d is its thickness, U_{FB} is flat-band voltage, $j=qN_a W^2/2\epsilon_s$ is interface potential in the depletion approximation, ϵ_s is semiconductor permittivity.

If we suppose that the total high-frequency capacitance is $C=(C_d^{-1}+C_s^{-1})^{-1}$ and $C_s = \epsilon_s/W$ then equation (6) can be expressed by observable C as

$$U_g = U_{FB} + \frac{1}{2} q N_a \epsilon_s a \left[\left(\frac{1}{C} - \frac{b}{C_d} \right)^2 - \frac{1}{a C_d^2} \right] \quad (7)$$

where $a=1+C_{ss}/C_d$ and $b=1-1/a$. The equation (7) is nonlinear $U_g(C^{-1})$ dependence with three parameters - U_{FB} , N_a and N_{ss} . In simple case, omitting N_{ss} and putting $a=1$, $b=0$, the equation (7) gives a well known relation $U_g \sim C^{-2}$. From the equation (7) it is evident that the most important term that affects C-V curve is C^{-1} , however, the C^{-2} term is not negligible though less meaningful. It means that only the multiple $N_a a$ can reliably be deduced from fitting.

TABLE I. The values of the accumulation capacitance C_d (recalculated also per unit area of the gate C_d/S), acceptor density N_a , and interface state density N_{ss} as calculated from the C-V dependences numbered from 1 to 4 in Fig.4. The interface state density of the dependence no. 3 was taken as zero for the reference. Omitted values could not be evaluated.

no.	C_d (pF)	C_d/S (nFcm ⁻²)	N_a (cm ⁻³)	N_{ss} (cm ⁻² eV ⁻¹)
1	76	3.2	2.6×10^{14}	4.7×10^{10}
2	84	3.6	1.0×10^{14}	1.5×10^{10}
3	95	4.0	0.6×10^{14}	0
4	64	2.6	---	---

The values of the accumulation capacitance C_d , acceptor density N_a and interface state density N_{ss} as calculated from the C-V dependences numbered from 1 to 4 in Fig.4 are presented in Table I. The calculation was made under the assumption that the interface state density of the C-V curve no. 3 is zero. Thus the results presented give the comparison of the absolute values changes but not the absolute values of the density of states themselves. The Fermi energy of the semiconductor E_F , surface potential j_s , flat-band voltage U_{FB} , and trap energy E_t calculated from Fig.4 are summarized in Table II.

The DLTS spectra performed on PS/c-Si structure are shown in Fig.5. We suppose that the dominant process leading to the disappearance of the C-V curve hysteresis after illumination of the sample is the trapping of the photoelectrons by a Si-H⁺ or even larger defect complex.

TABLE II. The Fermi energy of the semiconductor E_F , surface potential j_s , flat-band voltage U_{FB} , and trap energy E_t which could be evaluated from Fig.4.

no.	E_F (eV)	j_s (V)	U_{FB} (V)	E_t (eV)
1	0.25	---	3.8	---
2	0.32	0.20	1.1	0.525
3	0.34	0.16	-1.3	0.499

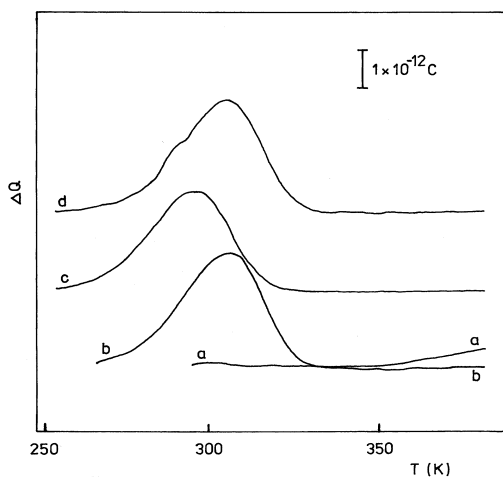


Fig. 5. DLTS spectra of PS/c-Si structures - (a) virgin sample, (b) after the 1st DLTS run, (c) after the 2nd DLTS run, (d) returned back to the state given by the curve (b). Discrete deep levels identified from the curve (c) correspond to that determined from the C-V curves.

Si- H^+ complex in a-Si:H semiconductor is usually denoted as D^+ or D^h . The light-soaking experiments with p-type Si:H/crystalline Si structure have given the evidence of the same effect – a subsequent decrease of the D^+ defect density on illumination⁴.

4. Conclusions

It can be concluded that the dominant process leading to the suppression of the large C-V hysteresis after the illumination of the PS/c-Si sample is the trapping of photoelectrons by Si- H^+ defects and their subsequent neutralization. A discrete trap deep level was created at the PS/c-Si interface with the thermal activation energy of 0.5 eV. The deep states are recovered in dark and their density N_{ss} is increased by $\sim 4.7 \times 10^{10} \text{ cm}^{-2} \text{ eV}^{-1}$.

Acknowledgements

This work was partially supported by Slovak Grant Agency VEGA (project no. 2/5081/98), by TEROSIL Inc., Rožn ov pod Radhořtem Czech Republic, and by Slovak Powerplants, Inc.

References

- [1]. A.G. Cullis, L.T. Canham, and P.D.J. Calcot, J. Appl. Phys. **82**, 909 (1997).
- [2]. R.C. Anderson, Ph.D.Thesis, Lawrence Berkeley Laboratory, University of California (1991).
- [3]. T.M. Bhave, S.V. Bhoraskar, P. Singh, and V.N. Bhoraskar, Nucl. Instr. Methods B **132**, 409 (1997).
- [4]. V. Nádař dy, R. Durný, I. Thurzo, and E. Piněřk, J. Non-Cryst. Solids **227-230**, 316 (1998).